Sonographic Mapping of the Normal Brachial Plexus

Xavier Demondion, Pascal Herbinet, Nathalie Boutry, Christian Fontaine, Jean-Paul Francke and Anne Cotten

AJNR Am J Neuroradiol 2003, 24 (7) 1303-1309
http://www.ajnr.org/content/24/7/1303

AJNR Am J Neuroradiol 24:1303–1309, August 2003

Sonographic Mapping of the Normal Brachial Plexus

Xavier Demondion, Pascal Herbinet, Nathalie Boutry, Christian Fontaine, Jean-Paul Francke, and Anne Cotten

BACKGROUND AND PURPOSE: **Mapping of the brachial plexus with MR imaging has been reported and may have potential clinical applications (eg, precise localization of traumatic or tumoral nerve lesions, selective anesthesia of the brachial plexus). We sought to demonstrate that mapping of the brachial plexus may be performed by means of sonography.**

METHODS: **Twelve healthy adult volunteers (seven women and five men; age range, 24–38 years; mean, 31 years) underwent bilateral sonographic examination for the assessment of the nerve structures of the brachial plexus from the extraforaminal part to the axillary part. Four formolated cadavers (two male and two female; age range, 66–84 years; mean, 77.5 years) were frozen and sawed into 3-mm-thick contiguous sections in the same plane as that used for the sonographic exploration.**

RESULTS: **A satisfactory sonographic examination was performed in 10 of 12 volunteers, leading to a good association with anatomic sections. Two volunteers were excluded from the study because a clear depiction of the brachial plexus was difficult owing to a short neck and low echogenicity at examination. The association between sonographic images and anatomic sections allowed us to map the brachial plexus. The subclavian and deep cervical arteries were useful landmarks for this mapping. The eighth cervical nerve root and the first thoracic nerve root were the most difficult part of the brachial plexus to depict because of their deep location.**

CONCLUSION: **The brachial plexus can be mapped with sonography. However, this technique requires a good grounding in anatomy and may be impossible in short-necked individuals.**

The brachial plexus is formed by the union of the anterior branches of the four lower cervical and first thoracic nerves. It extends from the lateral part of the cervical spine to the axilla. The upper trunk is classically formed by the joining of roots C5 and C6. The middle trunk is the continuation of root C7. The lower trunk is formed by the joining of roots C8 and T1. The three trunks are formed at the lateral border of the interscalene triangle. Each trunk divides into an anterior and a posterior division. The lateral cord is formed by the anterior divisions of the upper and middle trunks and the medial cord by the anterior division of the lower trunk. The posterior cord is formed by the posterior divisions of all the trunks. Just lateral to the pectoralis minor muscle, the cords divide into the five terminal branches (median nerve, ulnar nerve, musculocutaneous nerve, axillary nerve, and radial nerve) (Fig 1) (1).

Visualization of the brachial plexus by means of sonography has been reported (2–4), but thanks to the recent progress of sonography with high-frequency probes and postprocessing, a precise analysis of the course of the brachial plexus can be accurately assessed. To our knowledge, precise mapping of the brachial plexus during its course in the cervicothoracic-brachial junction (thoracic outlet) from nerve roots to nerve cords by means of sonography, with sonographic-anatomic comparison, has not been reported. In a study comparing sonography and MR imaging of the brachial plexus in five volunteers, Sheppard et al (3) indicated that they did not attempt, nor was it their intention, to identify all the components of the brachial plexus because these components are not usually distinguished with conventional MR imaging. However, since then, such MR mapping has been reported (5). Moreover, Sheppard et al (3) indicated that they could not examine the C7 and C8 roots. Finally, they used a 5–10 Hz transducer, which may not be the most appropriate one for the study of the brachial plexus. In a recent article, Martinoli et al

Received August 28, 2002; accepted after revision February 12, 2003.

From the Service de Radiologie Ostéo-Articulaire, Hôpital Roger Salengro (X.D., P.H., N.B., A.C.), and the Laboratoire d'Anatomie, Faculté de Médecine, (X.D., C.F., J.P.F.), Lille, France.

Address reprint requests to Xavier Demondion, MD, Service de Radiologie Ostéo-Articulaire, Hôpital Roger Salengro, Chru de Lille, Boulevard du Pr. J. Leclercq 59037 Lille Cedex France.

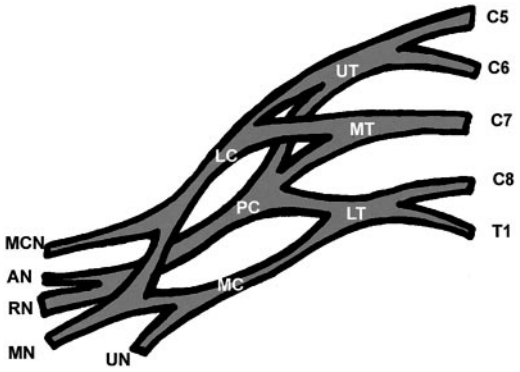

FIG 1. Schematic illustration of the different components of the right brachial plexus. *C5* indicates fifth nerve root; *C6*, sixth nerve root; *C7*, seventh nerve root; *C8*, eighth nerve root; *T1*, first thoracic nerve root; *UT,* upper trunk; *MT*, middle trunk; *LT*, lower trunk; *LC,* lateral nerve cord; *PC*, posterior nerve cord; *MC,* medial nerve cord; *MCN,* musculocutaneous nerve; *AN*, axillary nerve; *RN*, radial nerve; *MN*, median nerve; *UN*, ulnar nerve.

(6) reported a technique for assessing the roots by means of sonography, but they did not study the systematization of the trunks and cords of the brachial plexus.

The purpose of the current study was to demonstrate that mapping of the brachial plexus may be performed with sonography.

Methods

Between October 2001 and May 2002, twelve healthy adult volunteers (seven women and five men; age range, 24–38 years; mean, 31 years) underwent bilateral sonographic examination for the assessment of the nerve structures of the brachial plexus, from the extraforaminal part to the axillary part. The extraforaminal and interscalenic parts of the cervical nerve roots were assessed first. Then, the nervous structures were explored at the junction between the interscalene triangle and the costoclavicular space by a supraclavicular approach, and the costoclavicular space by an infraclavicular approach. Finally, exploration of the retropectoralis minor tunnel part of the nerve structures was performed. Written informed consent was obtained from each volunteer.

Sonographic images were obtained with a Sonoline Elegra scanner (Siemens Medical Systems, Iselin, NJ) with a high-frequency linear transducer, ranging from 10 to 13 MHz. The examinations were performed with the patient in a sitting position, with the head in neutral position. All the sonographic examinations were concomitantly performed by two radiologists (X.D., P.H.). Sonograms were obtained during each examination. The obliquity of the transducer at each compartment was identified by photographs taken during examination.

Then, four formolated cadavers (two male and two female; age range, 66–84 years; mean, 77.5 years) were used for comparison. The specimens were frozen at −40°C for at least 24 hours and subsequently sliced with a band saw into 3-mm-thick contiguous sections, in the same plane as that used for sonographic exploration. Photographs were obtained of each section.

For purposes of sonographic-anatomic comparison, the gross anatomic sections and the corresponding sonographic images were simultaneously interpreted in consensus by the two radiologists who had performed the sonographic examinations. The musculotendinous, nerve, vascular, and bone structures were identified on anatomic sections according to the descriptions found in the literature (1, 5, 7, 8) and compared with the sonograms.

Results

A satisfactory sonographic examination was performed in 10 of the 12 volunteers, leading to a good comparison with the anatomic sections. Two volunteers were excluded from the study because a clear depiction of the brachial plexus was difficult owing to a short neck (one case) or low echogenicity on examination (one case).

In each compartment, the nerve structures appeared as hypoechoic round to oval structures. Color Doppler sonography was used to differentiate nerve structures from vessels.

Extraforaminal Part

Sonography of the brachial plexus began with recognition of the cervical roots in their extraforaminal part. The probe was first positioned in the sagittal plane and then moved slightly outward and medially to study the cervical roots of the brachial plexus.

In each volunteer, the fifth, sixth, and seventh cervical roots were well visualized as they left the intervertebral foramina in a downward and outward direction (Fig 2). The fifth was found to be more oblique than the lower ones. The eighth cervical and first thoracic roots of the brachial plexus were more difficult to analyze because of their deep location. Another difficulty relating to these roots resulted from the concavity of the supraclavicular fossa, upon which the linear probe was difficult to apply. However, they were visualized in seven patients and united together soon after their exit to form a common trunk that was horizontal, or directed slightly upward. The deep cervical artery, which springs from the costocervical artery, was found to be helpful in distinguishing the eighth cervical root from the seventh, as it usually runs backward between these two nerve roots (7, 8) (Fig 3).

Interscalene Triangle

At the interscalene triangle, images were obtained in a sagittal plane (Fig 4A, Fig 5A). The interscalene triangle was well identified, bordered anteriorly by the anterior scalene muscle and posteriorly by the middle and posterior scalene muscles (Figs 4B and C, and 5B and C). In this space, the nerve structures appeared as oval hypoechoic structures arranged above the subclavian artery, which lies at the bottom of the interscalene triangle. Depending on the position of the probe, either the cervical nerve roots or their joining to form trunks were demonstrated. Once again, C8 and T1 (or the inferior trunk) were more difficult to visualize because of their deep location behind the subclavian artery. The systematization of the nerve structures was made possible by studying their continuity with the extraformaminal portion of the cervical roots.

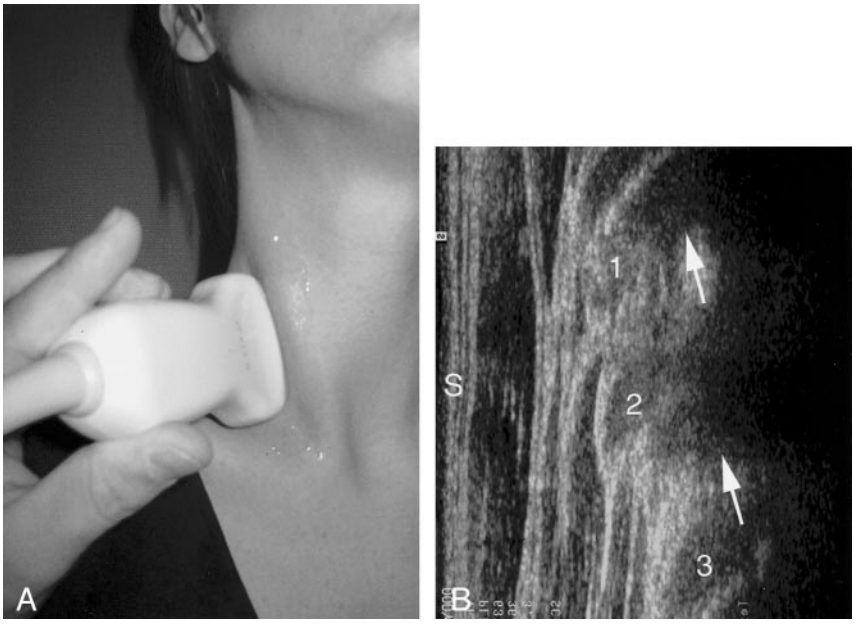

FIG 2. Cervical nerves roots at their extraforaminal part.

A, Position of the sonographic probe to explore cervical nerve roots at their extraforaminal part.

B, Sonogram (90° left rotated) in a 28-year-old female volunteer shows C5 (*1*), C6 (*2*), and C7 (*3*) roots at their extraforaminal part. They appear as oval hypoechoic structures. Note the shadowing of the cervical transverse processes (arrows). *S* indicates skin.

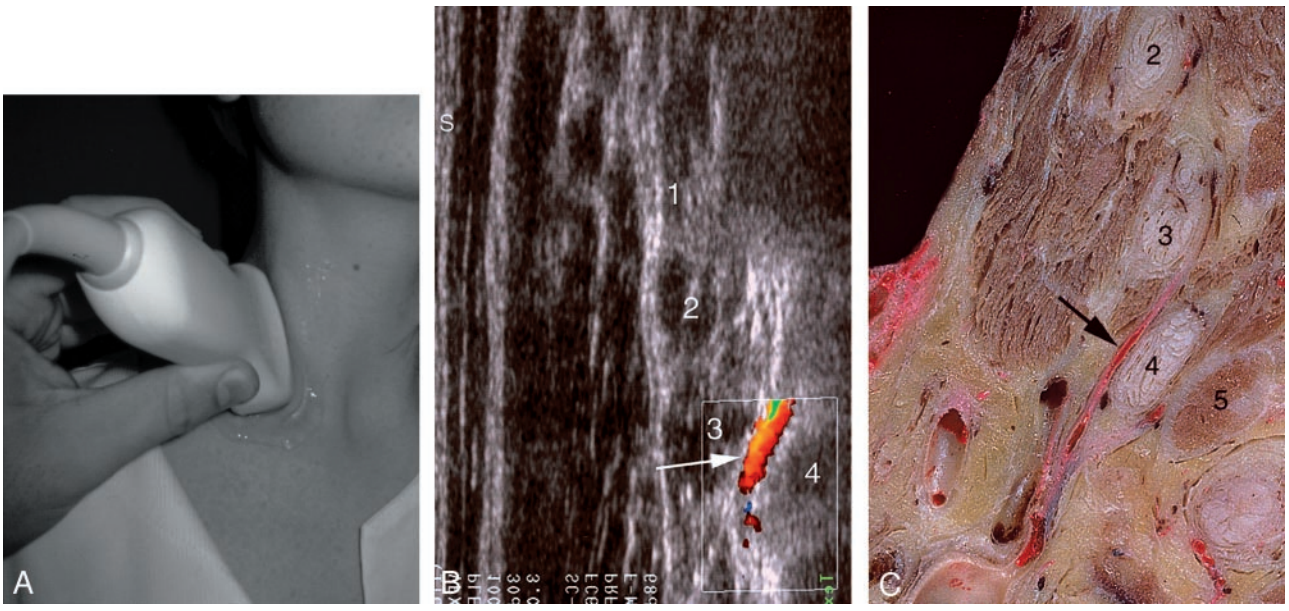

FIG 3. Relationship between the deep cervical artery and the C7 and C8 nerve roots.

A, Position of the probe to demonstrate the deep cervical artery.

B, Color Doppler sonogram (90° left rotated) in a 26-year-old female volunteer shows the deep cervical artery (arrow) separating the eighth cervical nerve (*4*) from the seventh (*3*).

C, Sagittal gross anatomic section shows the relationship between the deep cervical artery (arrow) and the C7 (*3*) and C8 (*4*) nerves roots.

In *B* and/or *C*, *1* indicates C5 nerve; *2*, C6 nerve; *5*, first rib; *S*, skin.

Junction Between the Interscalene Triangle and Costoclavicular Space

The supraclavicular region was assessed in a sagittal-oblique plane (the probe was slowly inclined medially and inferiorly) with the aim of identifying the brachial plexus at the junction between the interscalene triangle and the costoclavicular space (Fig 6A). In this region, the brachial plexus appeared as a triangular cluster of well-delineated round hypoechoic structures that represented the initial part of the cords, which resulted from the divisions of the trunks. They were located above the subclavian artery. The posterior cord was located at the highest point and the lateral cord in front of the medial cord (Fig 6B and C). These three cords could be clearly demonstrated in each volunteer.

Costoclavicular Space

This space could not be assessed directly because of the shadow of the clavicle; it was therefore explored by an infraclavicular approach (Fig 7A). With this

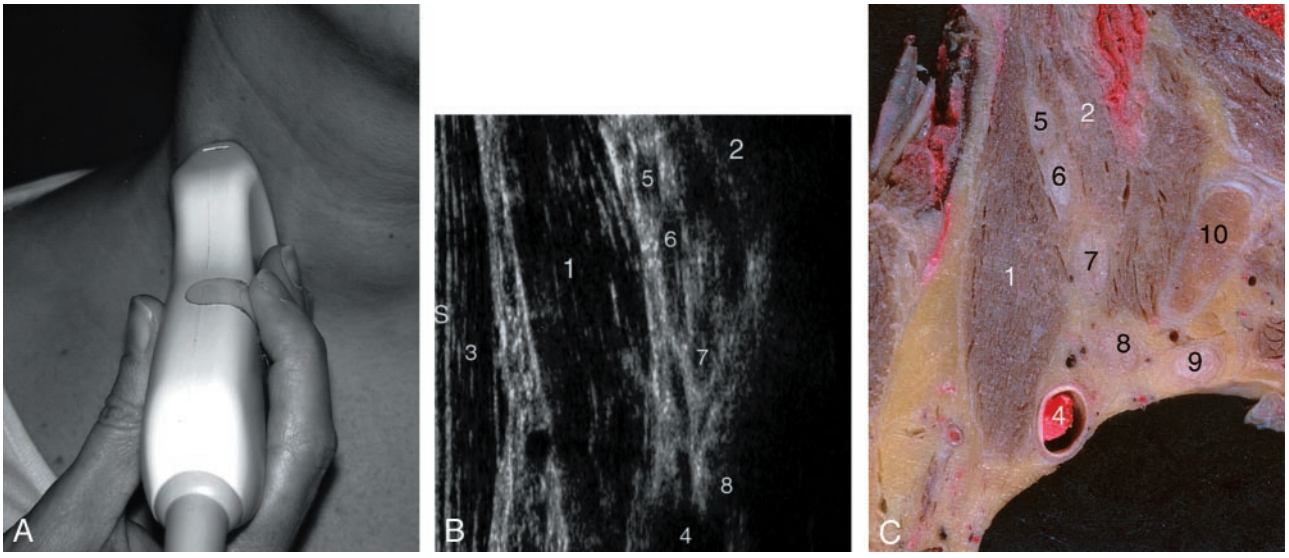

FIG 4. Interscalene triangle (nerves roots).
A, Position of the probe to explore the nerve roots at the interscalene triangle.
B, Sonogram (90° left rotated) in a 26-year-old female volunteer shows the C5 (*5*), C6 (*6*), and C7 (*7*) nerve roots at the interscalene triangle.
C, Sagittal gross anatomic section at the interscalene triangle.
In *B* and/or *C*, *1* indicates anterior scalene muscle; *2*, middle and posterior scalene muscles; *3*, sternocleidomastoid muscle; *4*, subclavian artery; *5*– *8*, C5 through C8 nerve roots; *9*, T1 nerve root; *10*, first rib; *S,* skin.

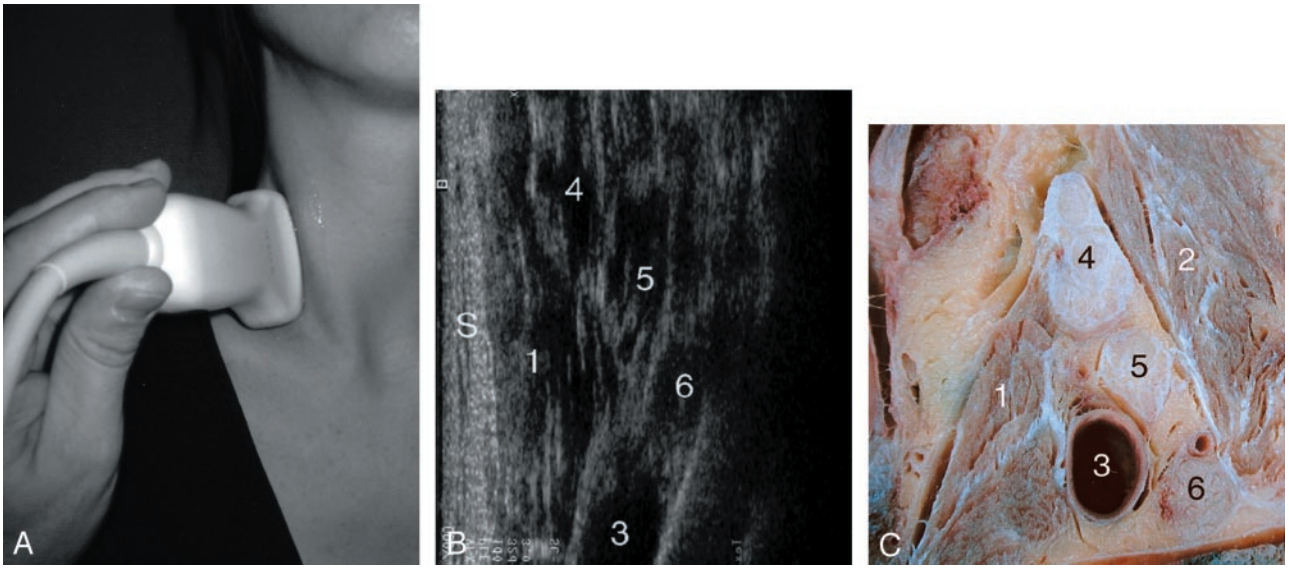

FIG 5. Interscalene triangle (trunks).
A, Position of the probe to explore the trunks at the interscalene triangle.
B, Sonogram (90° left rotated) in a 28-year-old male volunteer shows the upper, middle, and lower trunks at the interscalene triangle.
C, Sagittal gross anatomic section at the interscalene triangle (lateral part).
In *B* and/or *C*, *1* indicates anterior scalene muscle; *2*, middle and posterior scalene muscles; *3*, subclavian artery; *4*, upper trunk; *5*, middle trunk; *6*, lower trunk; *S*, skin.

approach, the limits of the costoclavicular space were the anterior rib cage posteriorly and the subclavius and pectoralis major muscles anteriorly. Within this triangular area, the subclavian artery and vein were well demonstrated, as were the cords of the brachial plexus located above and posterior to the subclavian artery. These sonographic incidences allowed fairly easy identification of all three cords of the brachial plexus, which showed a triangular arrangement in each volunteer (Fig 7B and C).

Space Behind the Pectoralis Minor

This space was well depicted by a sagittal plane (Fig 8A) bounded anteriorly by the pectoralis minor muscle, which is inserted into the coracoid process. The posterior limit of this deeply located space was difficult to demonstrate. Sonography allowed the cords of the brachial plexus to be visualized running parallel to the axillary vessels above and posterior to the axillary artery in each volunteer. In this space, the cords

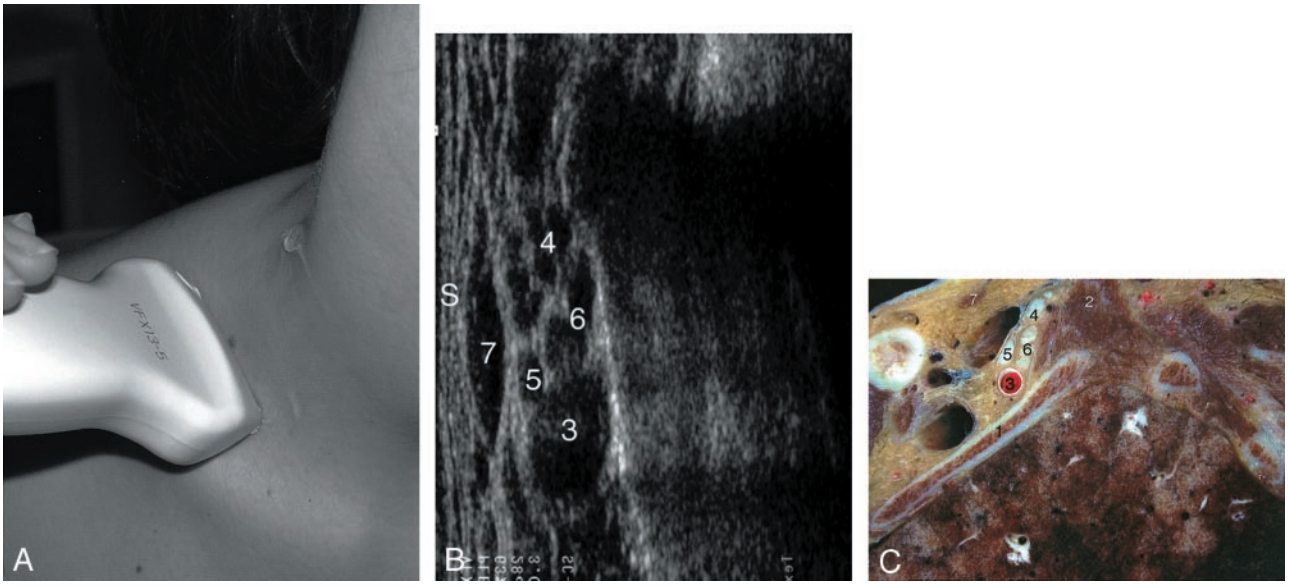

FIG 6. Junction between the interscalene triangle and the costoclavicular space (cords).
A, Position of the probe to explore the brachial plexus at the junction between the interscalene triangle and the costoclavicular space.
B, Sonogram (90° left rotated) in a 34-year-old male volunteer shows the nerve cords at the junction between the interscalene triangle and costoclavicular space.
C, Sagittal gross anatomic section at the junction between the interscalene triangle and costoclavicular space.
In *B* and/or *C*, *1* indicates first rib; *2*, middle and posterior scalene muscles; *3*, subclavian artery; *4*, posterior nerve cord; *5*, lateral nerve cord; *6*, medial nerve cord; *7*, omohyoid muscle; *S*, skin.

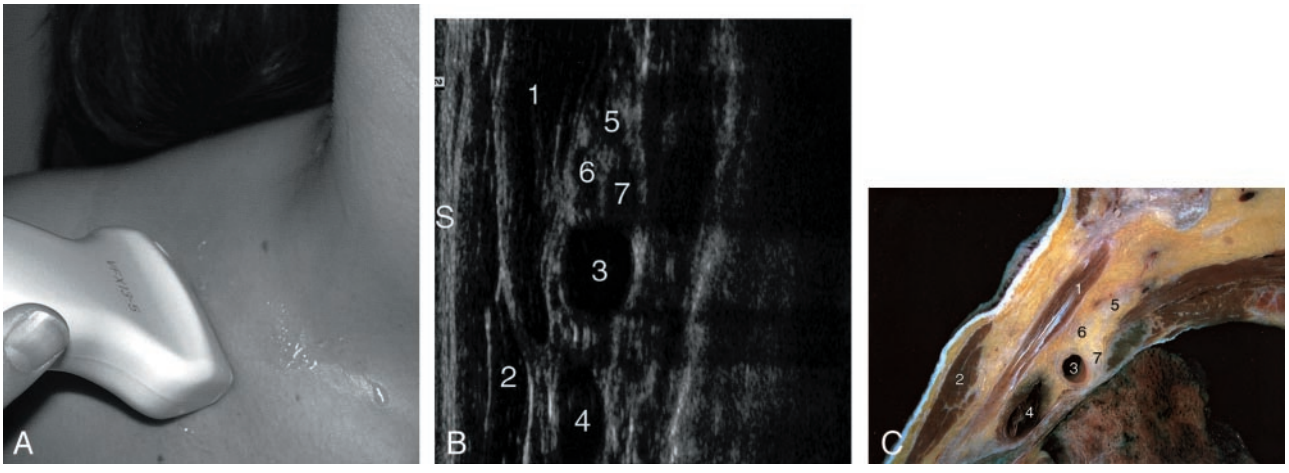

FIG 7. Costoclavicular space (cords).
A, Position of the probe to explore the brachial plexus at the costoclavicular space by an infraclavicular approach.
B, Sonogram (90° left rotated) in a 31-year-old female volunteer shows clusters of round hypoechoic neural fascicles of the different nerve cords at the costoclavicular space.
C, Sagittal gross oblique anatomic section of the costoclavicular space.
In *B* and/or *C*, *1* indicates subclavius muscle; *2*, pectoralis major muscle; *3*, axillary artery; *4*, axillary vein; *5*, posterior nerve cord; *6*, lateral nerve cord; *7*, medial nerve cord; *S*, skin.

maintained the same relationship as had been demonstrated in the costoclavicular space (Fig 8B and C).

Discussion

Visualizion of the brachial plexus with sonography has already been reported (2, 3). In agreement with the findings of Sheppard et al (3), the various components of the brachial plexus showed a hypoechoic pattern unlike that of the peripheral nerves, which may appear as echogenic fibrillar structures (9, 10). However, this study demonstrates that mapping of the brachial plexus can be carried out in the various compartments of the cervicothoracic-brachial junction (interscalene triangle, costoclavicular space, and space behind the pectoralis minor) by means of sonographic images obtained in a sagittal or sagittal-oblique plane (Fig 9). We decided to study the brachial plexus in a sagittal plane to obtain sonograms perpendicular to its long axis and to demonstrate its relationship with the subclavian artery and adjacent muscles, as reported with MR imaging (5, 11, 12).

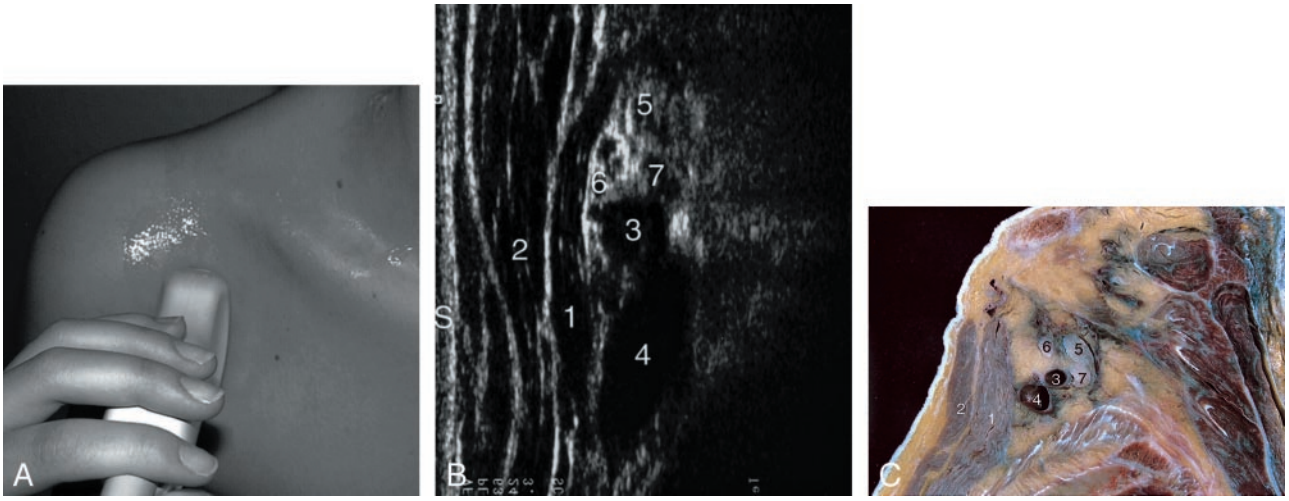

FIG 8. Retropectoralis minor space (cords).
A, Position of the probe to explore the brachial plexus at the retropectoralis minor space.
B, Sonogram (90° left rotated) in a 31-year-old female volunteer shows the nerve cords of the brachial plexus at the retropectoralis minor space.
C, Sagittal gross oblique anatomic section of the retropectoralis minor space.
In *B* and/or *C*, *1* indicates pectoralis minor muscle; *2*, pectoralis major muscle; *3*, axillary artery; *4*, axillary vein; *5*, posterior nerve cord; *6*, lateral nerve cord; *7*, medial nerve cord; *S*, skin.

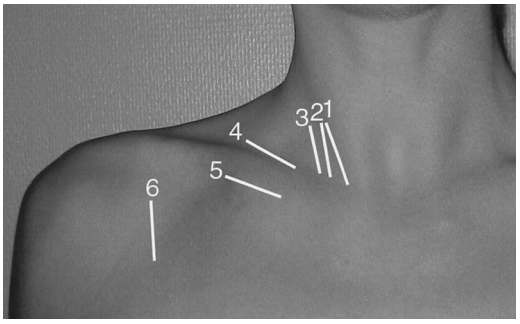

FIG 9. Schematic illustration indicates positioning of the probe to analyze *1*, the extraforaminal part of nerve roots and the deep cervical artery; *2*, the nerve roots at the interscalene triangle; *3*, the trunks of the brachial plexus; *4*, the cords of the brachial plexus by a supraclavicular approach; *5,* the cords of the brachial plexus by an infraclavicular approach; and *6*, the cords of the brachial plexus at the retropectoralis minor space.

When starting the sonographic examination of the various components of the brachial plexus, the subclavian artery may be localized by means of color Doppler ultrasonography or not. Indeed, this artery is an important landmark, as the brachial plexus is located just above it starting from the interscalene triangle.

Visualization of the extraforaminal part of the nerve roots and brachial plexus in the interscalene triangle was made possible by inclining the probe inferiorly and medially to a greater or lesser degree. The authors found that recognition of the C8 nerve root was facilitated by demonstration of the deep cervical artery, which runs backward habitually between the C7 and C8 nerve roots. Once the eighth cervical nerve root was identified, it was relatively easier to identify the other cervical roots of the brachial plexus. Recently, Martinoli et al (6) also proposed a technique for assessing the root level by using the differences in morphology of the cervical transverse processes: the anterior tubercle of the transverse process is selectively absent in the C7 vertebra. We did not attempt to use this technique in our study. These authors also outlined the difficulty in assessing the C8 and T1 nerves roots. They identified C8 in 80% of cases and the T1 nerve root in 40%. We agree that the assessment of C8 and T1 is difficult; in our study, we identified them in 58.5% of cases.

At the junction between the interscalene triangle and costoclavicular space, the cords were demonstrated as a cluster of hypoechoic round structures. This rather amazing appearance is due to the complexity of the divisions of the brachial plexus. However, continuity of the cords with the trunks could be demonstrated, allowing their systematization into posterior, lateral, and medial nerve cords. Moreover, the arrangement of the cords in this region has already been reported with MR imaging (5).

The costoclavicular space, which is often the site of vasculonervous compressions within the framework of the thoracic outlet syndrome, could not be directly demonstrated, as with MR imaging, because of the shadow of the clavicle. However, this compartment could be analyzed by a supra- or infraclavicular approach, which allowed the visualization of the posterior, medial, and lateral nerve cords of the brachial plexus in a triangular arrangement. This arrangement was maintained in the proximal part of the retropectoralis minor space.

Sonography thus appears to be a simple and inexpensive technique for the analysis of the brachial plexus. The knowledge of its precise mapping may have potential clinical applications. The usefulness of sonography in guiding percutaneous anesthesia has already been reported (2, 13), but selective anesthesia in the interscalene triangle, costoclavicular space, or

axillary space may be valuable. A precise assessment of nerve lesions in acute trauma or in primary or secondary tumors involving the brachial plexus may also represent a potential clinical application. Finally, mapping by sonography may be useful in dealing with the dynamically induced compression of the brachial plexus in patients with a neurogenic thoracic outlet syndrome. However, one of the limitations of this technique is the difficulty of visualizing the C8 and T1 nerve roots.

Conclusion

Sonography of the brachial plexus requires a good grounding in anatomy and appears difficult in short-necked individuals. We were able to recognize all the roots, trunks, and cords of the brachial plexus, with the exception of the C8 and T1 nerve roots in the extraforaminal region in three volunteers. Sonography thus appears to be an interesting tool for the assessment and mapping of the brachial plexus.

References

1. Gray H. Cervical nerves and brachial plexus. In: *Gray's Anatomy Descriptive and Surgical*, 10th ed. London: Longman, Green, and Co.; 1883:533–541
2. Yang WT, Chui PT, Metreweli C. **Anatomy of the normal brachial plexus revealed by sonography and the role of sonographic guidance in anesthesia of the brachial plexus.** *AJR Am J Roentgenol* 1998;171:1631–1636
3. Sheppard DG, Iyer RB, Fenstermacher MJ**. Brachial plexus: demonstration at US.** *Radiology* 1998;208:402–406
4. Guzeldemir ME, Ustonov B. **Ultrasonographic guidance in placing a catheter for continuous axillary brachial plexus block.** *Anesth Analg* 1995;81:882–883
5. Demondion X, Boutry N, Drizenko A, Paul C, Francke JP, Cotten A. **Thoracic outlet: anatomic correlation with MR imaging.** *AJR Am J Roentgenol* 2000;175:417–422
6. Martinoli C, Bianchi S, Santacroce E, Pugliese F, Graif M, Derchi LE. **Brachial plexus sonography: a technique for assessing the root level.** *AJR Am J Roentgenol* 2002;179:699–702
7. Gray H. **Subclavian artery.** In: *Gray's Anatomy Descriptive and Surgical*, 10th ed. London: Longman, Green, and Co.; 1883:364–378
8. Testut L. *Traité d'anatomie humaine.* Tome deuxième. Paris; Doin; 1929:260–283
9. Fornage BD. **Peripheral nerves extremities imaging with US.** *Radiology* 1988;167:179–182
10. Silvestri E, Martinoli C, Derchi LE, Bertolotto M, Chiaramondia M, Rosenberg I. **Echostructure of peripheral nerves: correlation between US and histological findings and criteria to differentiate tendons.** *Radiology* 1995;197:291–297
11. Blair DN, Sostman HD, Blair OC. **Normal brachial plexus: MR imaging.** *Radiology* 1987;165:763–767
12. Posniak HV, Olson MC, Dudiak CM, Wisniewski R, O'Malley C. **MR imaging of the brachial plexus.** *AJR Am J Roentgenol* 1993;161:373–379
13. Kapral S, Kraft P, Eibenberger K, et al. **Ultrasound-guided supraclavicular approach for regional anesthesia of the brachial plexus.** *Anesth Analg* 1994;78:507–513